IOPscience iopscience.iop.org

Home Search Collections Journals About Contact us My IOPscience

ENDOR studies on the W7 di-nitrogen centre in brown diamond

This article has been downloaded from IOPscience. Please scroll down to see the full text article.

1991 J. Phys.: Condens. Matter 3 3591

(http://iopscience.iop.org/0953-8984/3/20/020)

View the table of contents for this issue, or go to the journal homepage for more

Download details:
IP Address: 171.66.16.147
The article was downloaded on 11/05/2010 at 12:07

Please note that terms and conditions apply.

J. Phys.: Condens. Matter 3 (1991) 3591–3603. Printed in the UK

ENDOR studies on the W7 di-nitrogen centre in brown diamond

M E Newton† and J M Baker
Clarendon Laboratory, Parks Road, Oxford OX1 3PU, UK

Received 13 August 1990, in final form 29 January 1991

Abstract. A new technique, involving rapid and repeated sweeping of radio-frequency irradiation through a wide frequency range, has been used to enhance the ENDOR signal of the W7 di-nitrogen centre in diamond. This allowed the determination of the following magnetic hyperfine and electric quadrupole interaction parameters (expressed in MHz) for the two nitrogen atoms: $A_{\parallel}^{(1)} = 121.39(3)$, $A_{\perp}^{(1)} = 86.00(3)$, $P_{\parallel}^{(1)} = 2.55(3)$, $P_{\perp}^{(1)} = 1.27(3)$, $A_1^{(2)} = 13.58(5)$, $A_2^{(2)} = 16.01(5)$, $A_3^{(2)} = 14.00(5)$, $P_1^{(2)} = 0.13(1)$, $P_2^{(2)} = -0.13(1)$, $P_3^{(2)} = 0.000(5)$. The interactions for $\mathbf{A}^{(1)}$ and $\mathbf{P}^{(1)}$ are axially symmetrical about ⟨111⟩, but those for $\mathbf{A}^{(2)}$ and $\mathbf{P}^{(2)}$ have low symmetry, and their principal axes have no clear relationship with one another or with the crystal structure. Hence, the overall symmetry of the site is established as C_1.

1. Introduction

Nitrogen is a very common impurity in natural diamonds, which is thought to be incorporated substitutionally, and is sometimes present in excess of 1000 ppm. Unlike in synthetic diamonds, where most nitrogen appears as single substitutional atoms, the nitrogen in natural diamonds is far from statistically distributed over the substitutional sites. Quite high concentrations have been found of clusters involving several nitrogen atoms; for example in the diamond we have used in the investigation described in this paper, the concentration of centres involving more than one nitrogen atom is larger than that of single substitutional sites (see e.g. section 2).

Natural diamonds are found with a range of different colours. The (smoky) brown diamonds deserve attention by virtue of their special physical properties. Brown diamonds are characterized as type Ia by infrared absorption. They typically contain large amounts of nitrogen, most of which is incorporated in three types of defect: A- and B-centres and platelets (Davies 1977a, b, Berger and Pennycook 1982).

Brown diamonds contain high dislocation densities, with considerable disorder in the structure of the dislocations. Brown diamonds all bear traces of plastic deformation. Typically brown diamonds give rise to complicated irregular birefringence patterns, indicating large and irregular internal strain. When birefringence is observed through a (100) face, one often observes a system of intersecting lines which

† Present address: Medical College of Wisconsin, National Biomedical Research Center, 8701 Watertown Plank Road, Milwaukee, WI 53226, USA.

0953-8984/91/203591+13$03.50 © 1991 IOP Publishing Ltd

pass through one another, and so cannot be boundaries of growth planes (Wilks and Wilks 1987). These indicate {111} slip planes. Cathodoluminescence (CL) studies (Wilks and Wilks 1987) show that the growth of the brown diamonds must have been a very irregular process, whereas good quality natural diamonds grow in a regular octahedral habit.

Several EPR centres have been found in brown diamond, some of which are peculiar to brown diamond, and none of them has been unequivocally modelled. One of these is the W7 centre, discovered by Loubser and Wright (1973). It is a di-nitrogen centre with $S = \frac{1}{2}$, in which the two nitrogen atoms are not equivalent. The EPR measurements of Loubser and Wright (1973) have shown that one of the nitrogen atoms has hyperfine parameters similar to those of the P1 centre (Smith *et al* 1959), whilst the unpaired electron interacts only weakly with the second nitrogen; their spin Hamiltonian parameters are given in table 1 (the spin Hamiltonian is given in section 4.1, equation (1)). The W7 centres are not isotropically distributed over all possible symmetry-related sites allowed by the diamond structure.

Table 1. Spin Hamiltonian parameters for W7 measured by EPR at 77 K (Loubser and Wright 1973).

g	2.0028
$A_{\parallel}^{(1)}/h$	123.8 MHz principal direction [111]
$A_{\perp}^{(1)}/h$	87.5 MHz
$A_{\parallel}^{(2)}/h$	15.6 MHz principal direction [$\bar{1}$11]
$A_{\perp}^{(2)}/h$	13.2 MHz

This paper describes the application of the technique of ENDOR to the W7 centre, in order to get more detailed information about the hyperfine interactions and to measure the quadrupole interactions, so as to be better able to construct a model for the centre. Previously, detailed ENDOR investigations have been made only for centres involving one nitrogen, namely P1 (Cook and Whiffen 1966), N3 (van Wyk 1988) and OK1 (Newton and Baker 1989). The present paper describes the first detailed ENDOR investigation of a centre involving more than one nitrogen. Accurate values of the hyperfine and quadrupole interactions of W7 are determined. These show that the symmetry of the hyperfine interaction for $\mathbf{A}^{(2)}$ given in table 1 was incorrectly determined by EPR, presumably because of the small anisotropy. This new information is used in the next paper (Newton and Baker 1991, hereafter referred to as II) to differentiate between several models which have previously been proposed for the W7 centre.

2. Characterization of the diamond studied

The brown diamond used for our study of the W7 centre was a large irregular rounded dodecahedron, whose coloration was very inhomogeneous. The infrared (IR) absorption spectrum measured for this diamond is shown in figure 1. In diamond, the IR absorption in the one-phonon region is primarily due to the A, B and P1 nitrogen defects already discussed. Our experimental spectrum was reconsructed using a suitable

admixture of IR absorption spectra from IaA, IaB and synthetic Ib diamonds (diamonds containing only A, B or P1 centres respectively). This process indicated that the diamond we studied is in fact IaA, with only a small fraction of the IR absorption being due to P1 centres. Using correlation coefficients between the IR absorption and the A and P1 concentrations (Woods *et al* 1990, Chrenko *et al* 1971), we determined the approximate nitrogen concentration in the A and P1 centres as 270 and 30 ppm respectively (there was no observable concentration of B centres).

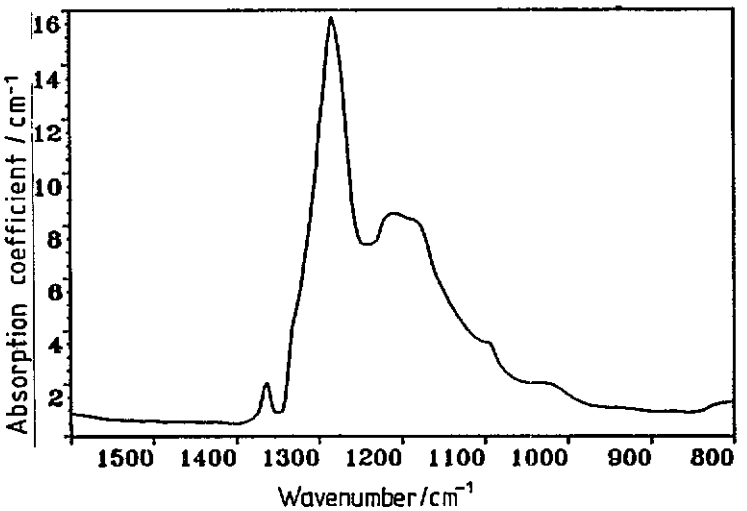

Figure 1. Infrared absorption spectrum in the one-phonon region of the brown diamond used in our study of the W7 centre.

When the diamond was viewed between crossed polaroids in white light, an irregular coloured birefringence pattern could be observed which is typical of heavily strained brown diamonds. Nomarski or Differential Interference Contrast Microscopy was used to study a natural surface of the diamond, and revealed a system of intersecting lines which indicate {111} slip planes. It is clear that the diamond has undergone significant plastic deformation.

3. Experimental techniques

3.1. Orientation of the sample

The approximate orientation of the sample, when it was glued to the holder for insertion in the EPR and ENDOR spectrometer, was determined by x-ray diffraction. For precise determination of the orientation, we used the EPR and ENDOR of the P1 centres present in the diamond. The P1 centre is a single substitutional nitrogen atom for which Jahn–Teller distortion produces a unique N–C bond containing a singly occupied anti-bonding orbital: an alternative description is of a lone pair on N and the unpaired electron mainly on C. There is a statistical distribution of centres over four such sites with axial symmetry about {111} directions. At room temperature and below, the EPR and ENDOR of this set of symmetry-related sites with well documented spin Hamiltonian parameters, enables one to use the spectra to determine the orientation of the applied magnetic field $\boldsymbol{B}$ in the crystal.

3.2. Conventional CW-ENDOR

Details of the ENDOR spectrometer, which operates at a microwave frequency of 9.3 GHz, have been given by Newton and Baker (1989).

Partial saturation of the CW-EPR is necessary for the observation of CW-ENDOR. However, if the EPR signal is too strongly saturated, the EPR signal-to-noise ratio may be so low that CW-ENDOR cannot be detected. Saturation can be reduced by reducing the microwave power; but, for signals which saturate easily, such low power levels may be necessary to avoid over-saturation that the sensitivity of a spectrometer incorporating homodyne detection may be degraded. EPR saturation can also be reduced by increasing the temperature; however, other experimental requirements, such as maximization of the CW-ENDOR effect, often requires measurement at low temperature.

Initially, attempts were made to use conventional double modulation methods to detect CW-ENDOR of W7 centres. The external magnetic field was modulated at 115 kHz to minimize detector noise, and the RF at the ENDOR frequency was frequency modulated at an audio frequency in the range 20–1000 Hz. The ENDOR was stored after double demodulation, and a number of sweeps through the range of ENDOR transitions was averaged to increase further the signal-to-noise ratio.

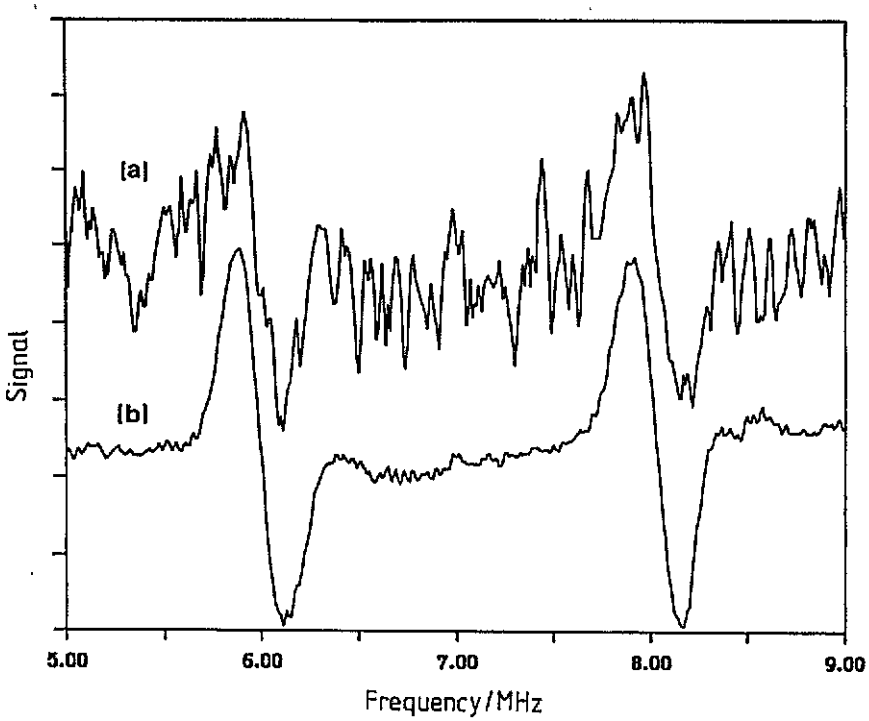

Figure 2. ENDOR spectrum of the minor nitrogen in W7 taken at 3.7 K: (*a*) using standard double modulation CW-ENDOR, and signal averaging 20 sweeps; and (*b*) with transient RF enhancement, and signal averaging for three sweeps.

ENDOR could be detected only at temperatures close to 4.2 K and the signal was very weak, even after considerable signal averaging: an example is shown in figure 2(*a*). Measurement was possible only along directions of high symmetry.

3.3. EPR and ENDOR using an RF enhancement technique

It was found, at temperatures below 77 K for EPR and below about 20 K for ENDOR, that the signals detected in the conventional way described in section 3.2 could be considerably enhanced if the sample was simultaneously irradiated with a second RF at about 50 W power level which was swept very rapidly and repeatedly in frequency through the ENDOR transitions.

Figure 3 shows an example of the enhancement of the EPR achieved in this way: the technical details of the experimental conditions are discussed in the appendix. Figure 4 shows the variation with temperature of this RF-induced enhancement of the EPR.

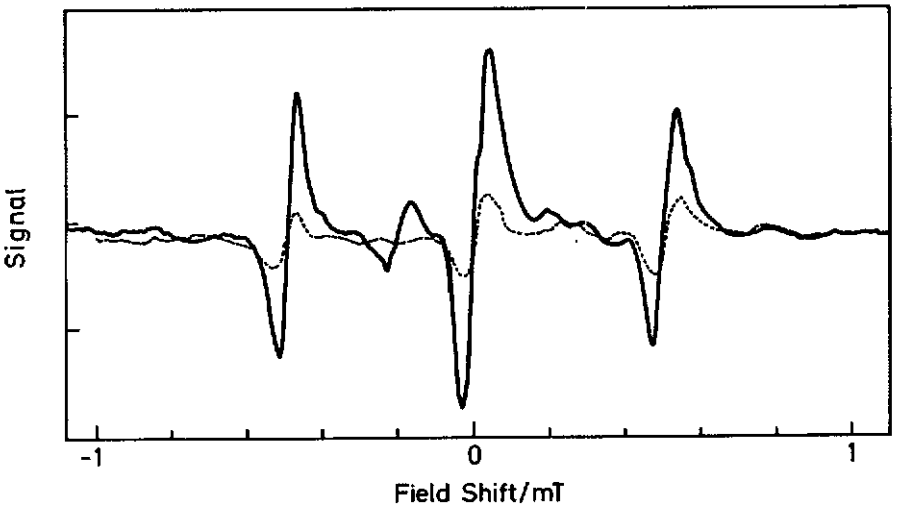

Figure 3. Part of the EPR spectrum of the W7 and P1 centres at 5 K for an arbitrary orientation of the magnetic field. The enhancement depicted was achieved by sweeping the RF over the range 40 to 65 MHz at approximately 1000 MHz s^{-1}. The RF power used was about 20 W, which was sufficient to saturate the nuclear transitions. The full trace shows the enhanced EPR and the broken trace the unenhanced EPR.

Figure 2(*b*) shows the improvement achieved in the signal-to-noise ratio of the CW-ENDOR achieved by this method, for which the technical details are discussed in the appendix. Improvements in the signal-to-noise ratio of the CW-ENDOR by an order of magnitude were achieved in this way. Only because of the enhancement of the ENDOR obtained in this way were we able to measure the angular variation of the ENDOR spectra of the two nitrogen atoms in the W7 centre which we describe later.

This enhancement technique also allowed the detection of ENDOR signals at higher temperatures than was possible with conventional CW-ENDOR.

3.4. The enhancement mechanism

The mechanism of the enhancement we observe is not fully understood. As the external magnetic field is being modulated, and both RF sources are being modulated, the spin packets are being swept through in a very complicated and ill defined way. As the EPR enhancement is produced by a very rapid sweep through the ENDOR transitions,

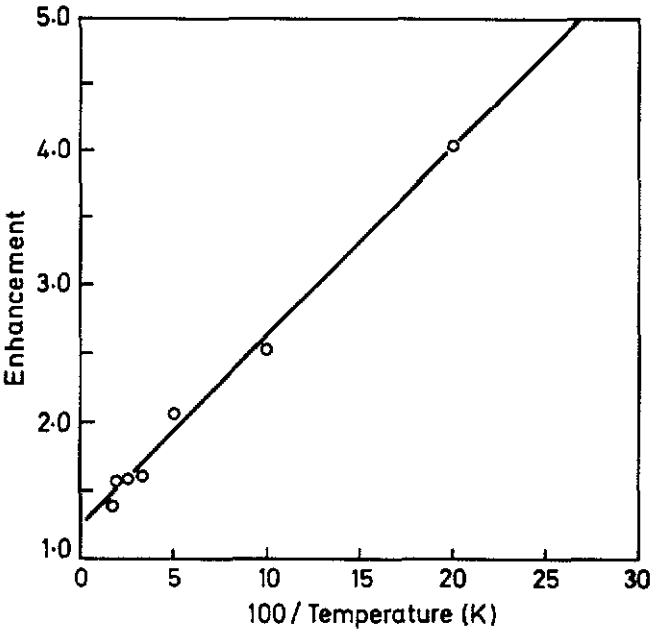

Figure 4. The ratio of peak-to-peak derivative EPR signal with and without enhancement as a function of reciprocal temperature for the $M_I^{(1)} = -1, M_I^{(2)} = 0$ transition of the W7 centre in diamond. The full line shows the best fit to a linear dependence.

it seems likely that it involves a transient ENDOR response. This is typically much greater than a CW-ENDOR response, but it lasts for a time shorter than T_{1e}. As we sweep repetitively through the transition, we may be integrating a succession of transient responses, which results in a larger signal than the heavily saturated CW response. Alternatively, we may be opening a succession of relaxation pathways, which increases the effective spin-lattice relaxation rate, and so reduces the level of saturation.

Since the CW-ENDOR signal-to-noise ratio depends on that of the EPR, the improvement in signal-to-noise ratio of the latter due to transient enhancement, is passed on to the CW-ENDOR in the experiment described in the previous section.

The technique previously described reduces the effective saturation of the EPR signal and, hence, facilitates operation at higher microwave powers, where the spectrometer performance is better. The technique has proved useful for the ENDOR investigation of many nitrogen defects in diamond including the OK1, P1 and N1 centres, as well as W7. The technique could usefully be applied for the study of other centres so long as T_{1e} is such that the EPR is strongly saturated, and the transient ENDOR enhancement occurs for attainable RF frequencies and sweep rates. As has been shown, the technique can result in significant improvements in CW-EPR and CW-ENDOR signal-to-noise ratios.

This CW-ENDOR enhancement technique is not equivalent to TRIPLE, from which it differs in three respects: (a) it gives a uniform enhancement across the ENDOR spectrum; (b) it gives a significant enhancement to the EPR signal; and (c) a rapid sweep of the second RF is necessary.

4. Results

4.1. EPR of the W7 centre

The complete spin Hamiltonian describing a centre with one unpaired electron, $S = \frac{1}{2}$, and two ^{14}N nuclei, $I^{(1)} = I^{(2)} = 1$, is:

$$H = \mu_B \boldsymbol{S} \cdot \mathbf{g} \cdot \boldsymbol{B} + \boldsymbol{S} \cdot \mathbf{A}^{(1)} \cdot \boldsymbol{I}^{(1)} + \boldsymbol{S} \cdot \mathbf{A}^{(2)} \cdot \boldsymbol{I}^{(2)} + \boldsymbol{I}^{(1)} \cdot \mathbf{P}^{(1)} \cdot \boldsymbol{I}^{(1)} + \boldsymbol{I}^{(2)} \cdot \mathbf{P}^{(2)} \cdot \boldsymbol{I}^{(2)} - g_N^{(1)} \mu_N \boldsymbol{I}^{(1)} \cdot \boldsymbol{B} - g_N^{(2)} \mu_N \boldsymbol{I}^{(2)} \cdot \boldsymbol{B} + \boldsymbol{I}^{(1)} \cdot \boldsymbol{J} \cdot \boldsymbol{I}^{(2)} \quad (1)$$

where μ_N is the nuclear magneton. It is not possible to determine all of the parameters from the EPR spectrum, but the full spin Hamiltonian is given here for reference both to this section and to section 4.2.

The EPR of W7 was first described by Loubser and Wright (1973), who gave the spin Hamiltonian parameters, measured at 77 K, listed in table 1. At 77 K there are only two similar spectra related by reflection symmetry in the (011) plane with axially symmetrical hyperfine matrices about [111] for $\mathbf{A}^{(1)}$ and [$\bar{1}$11] for $\mathbf{A}^{(2)}$ of one spectrum, and *vice versa* for the other; that is there is not the full range of symmetry-related sites one would expect for a crystal with the diamond structure. They also studied a motional averaging effect observed at temperatures above 77 K, and showed that the observed spectra could be accounted for by the 'hopping' of the unpaired electron between the two nitrogen atoms, thus exchanging their roles.

Slow motion takes place below about 200 K. As the temperature is raised, some hyperfine lines remain unchanged and others broaden and disappear quickly. Only those lines for which the electron sees the same effective field after the jump remain unchanged. At high temperature, a much simplified EPR spectrum is observed: typical spectra showing the motional averaging, are illustrated by Loubser and Wright. It should be noted that it is the central and outermost hyperfine lines which remain upon averaging: these must be lines corresponding to the same M_I quantum numbers for the two nitrogen nuclei $(+1,+1)$, $(0,0)$ and $(-1,-1)$, which indicates that the hyperfine interaction with both nitrogen nuclei has the same sign.

It is established from the previous EPR studies of Loubser and Wright (1973) and Shcherbakova *et al* (1975) that the larger of the two hyperfine interactions in W7 (the major hyperfine interaction) is similar in magnitude to that of the P1 centre, and is axially symmetrical about a ⟨111⟩ axis. This was confirmed in our measurements by comparison of the EPR and ENDOR spectra of P1 and W7 in the same sample when it was oriented in a plane close to a {110} plane. This plane was not the plane of reflection symmetry for the two W7 sites, so these measurements gave data for two different planes relative to each W7 centre. Figure 5 shows the angular variation of some of the lines in this plane. Once it had been confirmed that the major nitrogen hyperfine interaction in W7 is axially symmetric about a ⟨111⟩ direction, the exact orientation of the plane, and of $\boldsymbol{B}$ within it, were determined from the spectrum of the major nitrogen, whose spectrum was much stronger than that of P1 in our sample.

The EPR could be easily saturated at 4.2 K (the available microwave power was about 100 mW, but much less was required for saturation). The peak-to-peak EPR line width was about 50 μT. The spectra observed corresponded to centres whose major hyperfine axes were parallel to only two out of the four possible ⟨111⟩ directions. At X-band ($\sim$ 9 GHz) the centre of the spectrum of W7 is overlapped by the broad isotropic line of the N2 centre. In order to resolve the middle of the spectrum of W7

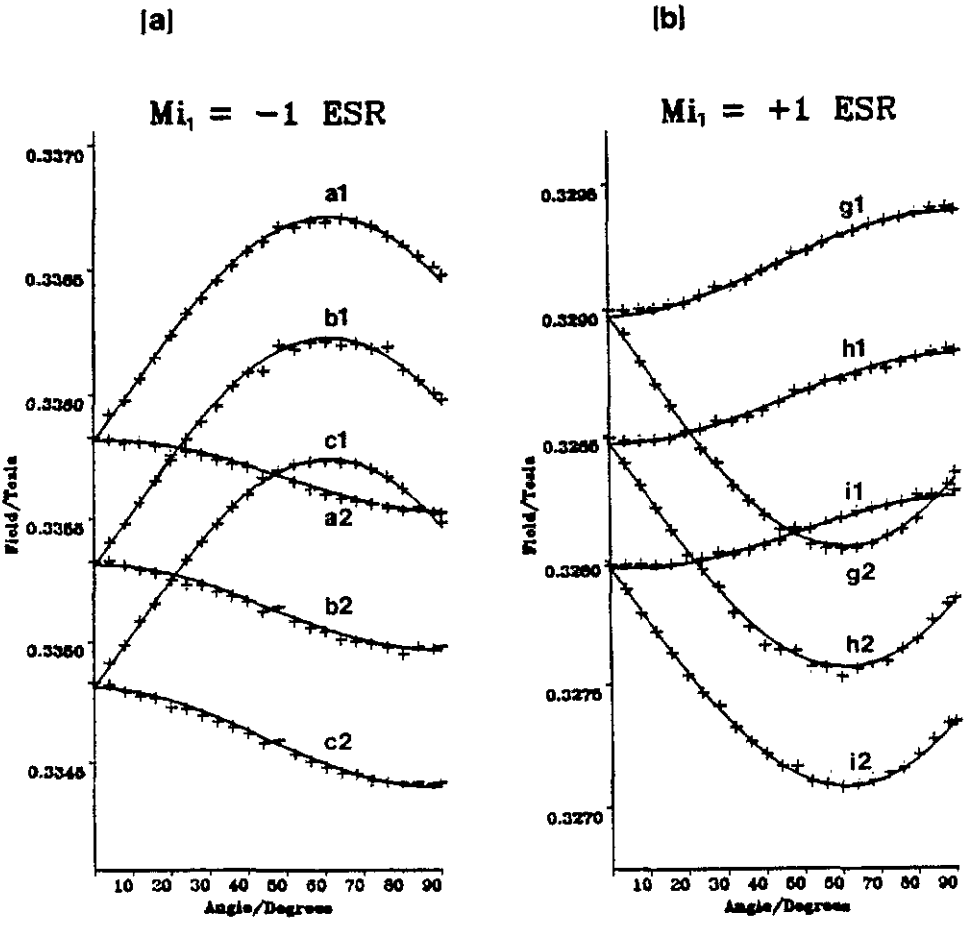

Figure 5. Angular variation of the EPR spectrum of W7 at 4.2 K and 9 GHz in a plane close to {110} for: (*a*) $M_I^{(1)} = -1$; (*b*) $M_I^{(1)} = +1$. The full curves are calculated using $g = 2.0023$ and the hyperfine and quadrupole interaction parameters determined from our ENDOR measurements.

from that of N2, measurements were made at the J-band ($\sim$ 17 GHz), which enabled us to measure accurately the electronic g-value of the W7 centre relative to that of the P1 centre. This g-value of the W7 centre is isotropic and equal to 2.0023(3); cf table 1.

4.2. ENDOR on the major nitrogen of the W7 centre

ENDOR measurements were made on the EPR transitions associated with $M_I^{(1)} = -1$, $M_I^{(2)} \simeq 0$ and $M_I^{(1)} = +1, M_I^{(2)} = 0$, labelled b1, b2 and h1, h2 respectively in figure 5. A very small amplitude of 115 kHz magnetic field modulation was used, less than the EPR line width, and the EPR was detected in dispersion. The RF frequency was modulated at 87 Hz. After double phase sensitive detection the output was stored for signal averaging. The method described in section 3.3. was used to enhance the EPR and ENDOR signals. The ENDOR line width is about 180 kHz. Over 200 ENDOR transitions were measured to determine the angular variation shown in figure 6: the full curves represent the calculated variation using the parameters which gave the best

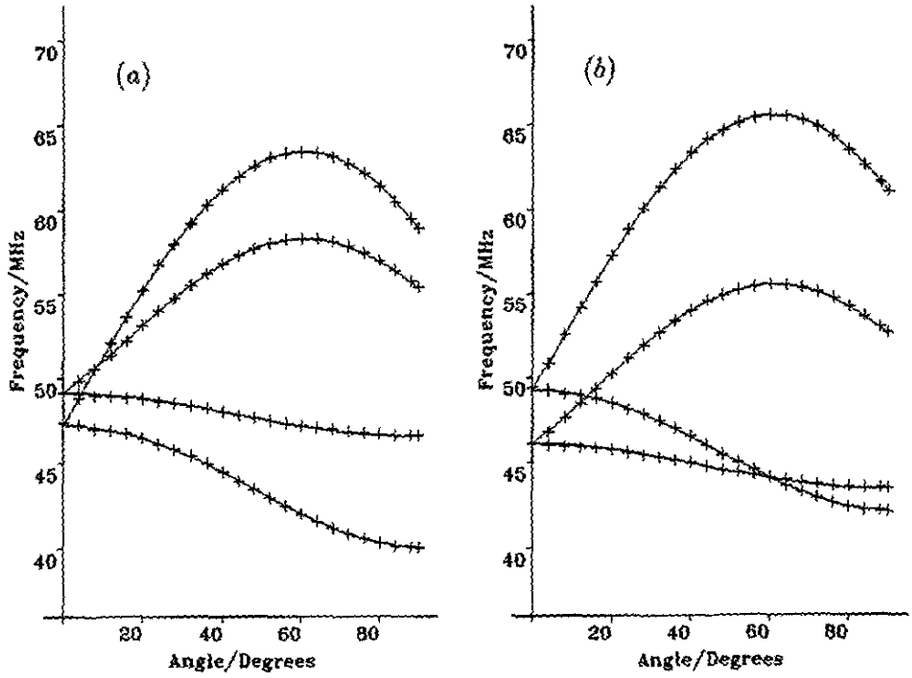

Figure 6. Angular variation of the ENDOR of the major nitrogen in a plane of known orientation close to a {110} plane for the EPR transitions corresponding to values of $[M_I^{(1)}, M_I^{(2)}]$: (a) [−1,0]; (b) [+1,0]. The full curves are calculated from the parameters determined by the best fit to the data.

fit in a least-squares analysis, using the theory outlined later.

The electronic g-factor was taken to be isotropic (section 4.1) and we assumed that g_N is isotropic. As coupling **J** between the two nitrogen nuclei is negligible, computer time was saved by exact diagonalization of the 6 × 6 matrices for each of the nitrogen nuclei interacting separately with the electron.

For the major nitrogen it was *assumed* that both $\mathbf{A}^{(1)}$ and $\mathbf{P}^{(1)}$ are axially symmetric about the same ⟨111⟩ direction. As the crystal was not oriented precisely in our spectrometer, the orientation of $\boldsymbol{B}$ in the crystal was regarded as unknown as well as the parameters $A_\parallel^{(1)}, A_\perp^{(1)}$, and $P_\parallel^{(1)}$ in a least-squares fitting procedure: initially g_N was treated as a variable to establish beyond doubt that ^{14}N is the nucleus involved, but for the final fit it was set at 0.4035.

The parameters obtained in this way are given in table 2. The orientation of the crystal plane was confirmed by the angular variation of the ENDOR of the P1 centre, which is known to be axially symmetrical. Relaxation of the constraint of axial symmetry for $\mathbf{A}^{(1)}$ and $\mathbf{P}^{(1)}$ did not affect the fit within the uncertainties of the parameters determined.

The hyperfine parameters may be factorized into an isotropic component A_s, and a traceless component A_p, arising from 2s-electron wavefunction ψ_{2s} and 2p-electron wavefunction ψ_{2p} respectively on the nitrogen atom, using $A_\parallel = A_s + 2A_p$ and $A_\perp = A_s - A_p$. Taking the unpaired electron to be in an orbital ψ with amplitude

Table 2. Spin Hamiltonian parameters for the major nitrogen in W7 determined by ENDOR.

Parameter	Value (MHz)	Direction of principal axis
$A_{\parallel}^{(1)}/h$	121.39(3)	[111]
$A_{\perp}^{(1)}/h$	86.00(3)	
$P_{\parallel}^{(1)}/h$	−2.55(3)	[111]
$P_{\perp}^{(1)}/h$	+1.27(3)	

η on the nitrogen atom, where

$$\psi = \eta(\alpha\psi_{2s} + \beta\psi_{2p})$$

one can use the hyperfine parameters to deduce the parameters η, α and β (Herman and Skillman 1963, Morton and Preston 1978). Table 3 gives the parameters deduced in this way, and compares them with the equivalent parameters for the P1 centre. It is seen that all parameters for W7 and P1 are very similar.

Table 3. ^{14}N hyperfine parameters and calculated molecular orbital coefficients for P1, and the major nitrogen of W7 centres: $p/s = \beta^2/\alpha^2$.

Centre	A_s/h(Mhz)	A_p/h(MHz)	α^2	β^2	η^2	p/s
P1[a]	92.22	10.88	0.206	0.794	0.247	3.85
W7	97.79	11.79	0.203	0.797	0.267	3.93

[a] Cook and Whiffen (1966).

4.3. ENDOR on the minor nitrogen of the W7 centre

The ENDOR transitions of the minor nitrogen lie in the range 5–10 MHz. Measurements were made using EPR lines for all values of $M_I^{(2)}$ for $M_I^{(1)} = \pm 1$, but the most detailed investigation was made for $M_I^{(1)} = 1, M_I^{(2)} = 0$, labelled h1 and h2 in figure 5. A typical ENDOR spectrum is shown in figure 2: the ENDOR line width was about 190 kHz. Over 200 transitions were measured in a plane close to {110} and over 50 in a plane close to {100}. The precise orientation of $\boldsymbol{B}$ in the crystal was determined from the accurately known spectrum of the major nitrogen. The angular variation in the plane close to {110} is shown in figure 7.

The same programme for least-squares fitting of the measured angular variation of the ENDOR spectrum of the minor nitrogen with predictions of a diagonalization of the matrix of the spin Hamiltonian, as was used for the major nitrogen, was used to obtain the spin Hamiltonian parameters listed in table 4. The precision with which the principal directions are determined is limited by the fact that the anisotropy is very small, and the number of spin Hamiltonian parameters to be fitted is large (12). Several fits were made with different subsets of data to estimate the uncertainty in the parameters. Great care was taken over this, both because our results for the minor nitrogen deviate from those found by previous authors, and because it turns out to be crucial in our model of the centre. The principal values of $\mathbf{A}^{(2)}$ found by Loubser and

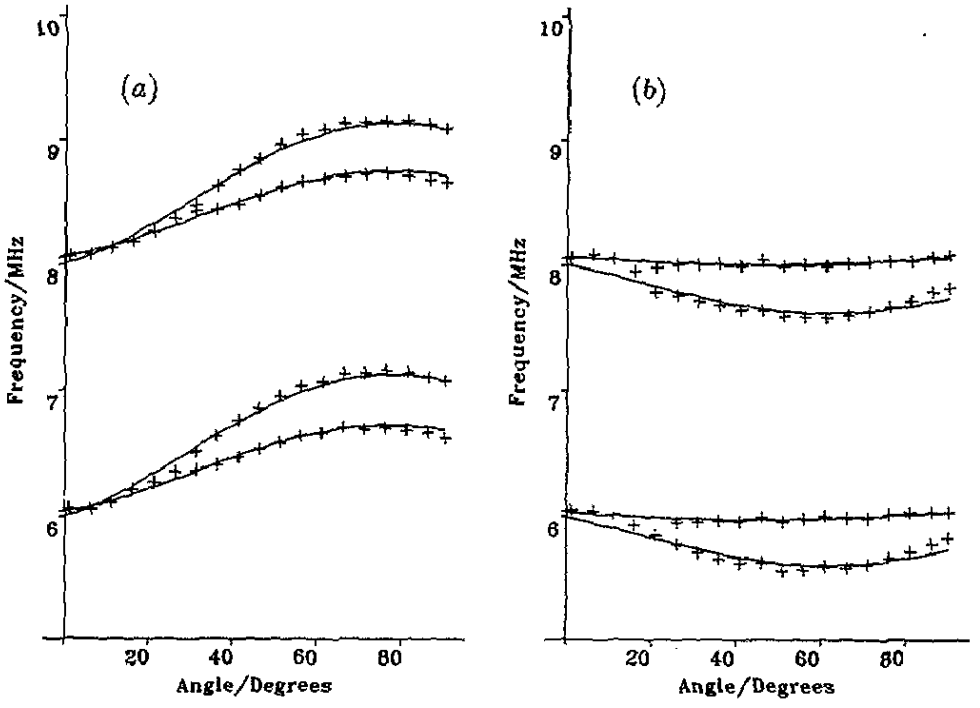

Figure 7. Angular variation of the ENDOR of the minor *nitrogen in a plane of known orientation close to a* {110} plane for the EPR transitions (*a*) h1 and (*b*) h2 labelled *on figure 4. The full curves are calculated from the parameters determined by the best fit to the data.*

Wright are given in table 1, showing axial symmetry; and for comparison with our results in table 4, the principal direction of $A_2^{(2)}$ is (0.8165, 0, 0.5774). The motional averaging at temperatures above 77 K showed that the signs of the A parameters are the same for the two nitrogen atoms.

Table 4. Spin Hamiltonian parameters for the minor *nitrogen in W7* determined by ENDOR. The direction cosines for the principal axes are expressed relative to $x[011], y[0\bar{1}1], z[100]$.

Parameter	Value (MHz)	Direction of principal axis		
$A_1^{(2)}/h$	13.58(5)	0.174(34)	0.866(18)	0.454(31)
$A_2^{(2)}/h$	16.01(5)	0.899(16)	−0.326(33)	0.292(17)
$A_3^{(2)}/h$	14.00(5)	−0.407(32)	−0.358(16)	0.839(9)
$P_1^{(2)}/h$	0.13(1)	−0.035(17)	0.875(27)	0.485(46)
$P_2^{(2)}/h$	−0.13(1)	0.956(17)	−0.122(52)	0.276(51)
$P_3^{(2)}/h$	0.000(5)	−0.292(50)	−0.469(46)	0.839(30)

The measured anisotropy of both magnetic hyperfine and electric quadrupole interactions is very small and the principal directions of $\mathbf{A}^{(2)}$ and $\mathbf{P}^{(2)}$ do not bear any clear relationship either to one another or to specific aspects of the crystal structure.

It seems unlikely that one can interpret such a small anisotropic hyperfine component in terms of a fraction of unpaired electron in an orbital on the nitrogen, as we did for the major nitrogen, because indirect contributions such as spin polarization may be of the observed magnitude.

5. Conclusion

ENDOR measurements on the W7 centre have shown that, although the magnetic hyperfine and electric quadrupole interaction matrices for the nitrogen atom with the larger interaction have axial symmetry about a ⟨111⟩ direction, these matrices for the other nitrogen atom have no symmetry: this result for the other nitrogen is in disagreement with the earlier EPR measurements of Loubser and Wright (1973). Hence, the overall symmetry of the W7 centre is C_1. This determination of the symmetry, together with other information about the centre, is used in the following paper (II) to determine an atomic model of the centre.

Acknowledgments

The authors are indebted to Professor J H N Loubser and Dr J A van Wyk for encouragement, advice and many helpful discussions. Grateful acknowledgment is made to Dr R J Caveney and De Beers Industrial Diamond Division for the provision of samples and a studentship for MEN.

Appendix. On the RF enhancement method

A1. Conditions for enhancement of the EPR

The RF signal which was swept rapidly through the ENDOR transitions was produced by a Hewlett Packard 8601A signal generator (output range 0.1 to 110 MHz), amplified by a broadband ENI 3100L amplifier, and fed to the broadband RF coil of a TM_{110} ENDOR cavity. The frequency of the RF signal generator was swept using a variable frequency sine wave oscillator. For frequency modulation frequencies up to 100 Hz it was possible to sweep the frequency of the 8601A signal generator over its entire range from 1 to 110 MHz.

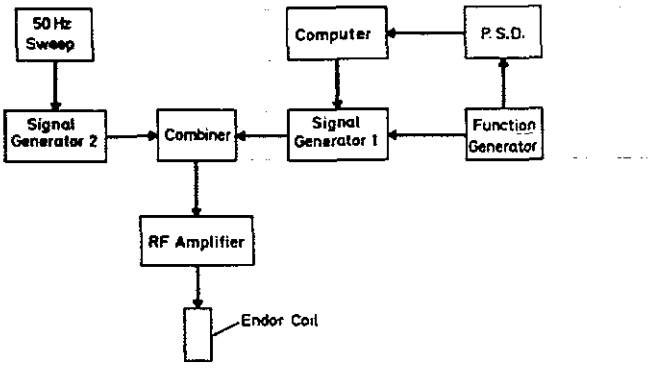

Figure A1. Block diagram showing the RF-ENDOR system.

A2. Conditions for enhancement of the CW-ENDOR

The RF system of a CW-ENDOR spectrometer was adapted to use the enhancement discussed in the previous section. A block diagram of the RF system is shown in figure A1. Signal generator 2 (RF2) was used to produce the EPR enhancement, and signal generator 1 (RF1) was used to stimulate steady state CW-ENDOR. Whilst enhancing the EPR with RF2, RF1 was swept slowly through the ENDOR transitions. RF1 was also frequency modulated at audio frequencies; hence at resonance, this modulation was passed to the EPR signal, which was also modulated at 115 kHz by the field modulation. Double phase sensitive detection was used to extract the CW-ENDOR signals.

References

Berger S D and Pennycook J 1982 *Nature* **298** 635
Chrenko R M, Strong H M and Tuft R E 1971 *Phil. Mag.* **23** 313
Cook R J and Whiffen D J 1966 *Proc. R. Soc.* A **295** 99
Davies G 1977a *Chem. Phys. Carbon* **13** 1
—— 1977b *J. Phys. C: Solid State Phys.* **9** L537
Herman F and Skillman S 1963 *Atomic Structure Calculations* (Englewood Cliffs, NJ: Prentice-Hall)
Loubser J H N and Wright A C J 1973 *J. Phys. D: Appl. Phys.* **6** 1129
Morton J R and Preston K F 1978 *J. Magn. Reson.* **30** 577
Newton M E and Baker J M 1989 *J. Phys.: Condens. Matter* **1** 10549
—— 1991 *J. Phys.: Condens. Matter* **3** 3605
Shcherbakova M Ya, Sobolev E V, Nadolinnyi V A and Aksenov V K 1975 *Sov. Phys.–Dokl.* **20** 725
Smith V W, Sorokin P P, Gelles I L and Lasher G J 1959 *Phys. Rev.* **115** 1546
van Wyk J A 1988 *Diamond Conf. (Cambridge)* p 125
Wilks E M and Wilks J 1987 *Wear* **118** 161
Woods G S, Purser G C, Mtimkulu A S S and Collins A T 1990 *J. Phys. Chem. Solids* **51** 1191